A Versatile Prognostics Approach for Batteries and Hydrogen Storage Systems Health Management

Théo Lenoir [1], Daniela Chrenko[1], Robin Roche[1], Samir Jemei[1], Mickaël Hilairet[2]
[1]Université Marie et Louis Pasteur, UTBM, CNRS, institut FEMTO-ST, FCLAB, F-90000 Belfort, France ; [2]Ecole Centrale de Nantes - LS2N, UMR CNRS 6004
[1]2 Rue Edouard Belin, 90000 Belfort, France ; [2]1, rue de la Noë, BP 92101, 44321 NANTES Cedex 3, France

E-Mail: theo.lenoir@utbm.fr

ACKNOWLEDGMENT

This work has been supported by the EIPHI Graduate School (contract ANR-17-EURE-0002) and the Region Bourgogne Franche-Comté. This work was supported by the French Research Agency under project ANR-22-CE05-0026.

***Index Terms*—Prognostics, state-of-health, batteries, fuel cells, electrolyzers.**

***Abstract*—The degradation of energy storage systems, including batteries, proton exchange membrane fuel cells, and electrolyzers, presents a critical challenge to their long-term reliability and efficiency. This study addresses the prediction of Remaining Useful Life by selecting a robust state-of-health indicator tailored to each system. A novel data-driven prognostic approach is proposed, leveraging Long Short-Term Memory neural networks to capture temporal dependencies and nonlinear degradation trends. The recurrent neural network model demonstrates versatility, adapting to both electrochemical storage and hydrogen-based systems by effectively learning from diverse datasets. Results highlight the method's capability to generalize across technologies, enabling accurate degradation predictions and offering significant insights into performance management.**

I. INTRODUCTION

With the development of intermittent renewable energies, the need for energy storage is growing [1]. Batteries and hydrogen storage offer flexible, decentralized solutions that are suitable for various applications, from mobility to stationary applications. Nevertheless, this approach has its share of drawbacks. Indeed, it is well-known that the electrical characteristics (capacity or power) of batteries deteriorate with operation [2]. Similarly, the proton exchange membrane (PEM) fuel cells and PEM electrolyzers needed for hydrogen-electricity conversion are seeing their power characteristics degrade over time [3][4]. Such damage can have serious consequences for the operation of a system using these storage components, since they may no longer be able to fulfill their role. This is the reason why diagnostic methods have recently been developed to quantify ageing. There are several different diagnostic approaches, depending on the system under study, but it is nevertheless common to seek to represent ageing in terms of a single indicator called state-of-health (SOH) [5][6]. Having this SOH indicator then allows to implement energy management strategies (EMS) that integrate the knowledge of the SOH to be more tolerant to ageing, on two different layers. Firstly, quantifying degradations allows for EMS to take into account the change in behavior and consequently have suited requirements. This is a rather reactive approach. On the other hand, EMS can also aim to reduce the ageing, in what would be a proactive approach. This proactive approach would be better if information about the potential SOH evolution in the future were to be known. It is in this context that prognostics are developed in the field of electrical storage components. Its aim is to predict future behavior of these elements, in order to adapt the power distribution between them. However, prognostic methods are usually applied to individual systems and often rely on simplistic techniques, such as linear extrapolation. In this context, a new method applicable to all storage systems would provide a unified approach for multi-source applications. Additionally, it could enable more accurate predictions by accounting for higher profile complexity. These are the primary objectives and key contributions of this work.

In that context, this paper will first present a short clarification of the SOH definitions. This will be followed by the adapted prognostics methodology, which should

be suitable to predict future behaviors of both batteries and hydrogen storage systems.

II. State-of-health definitions

To quantify ageing of storage components, state-of-health is first defined for each of them.

A. Batteries

The most common battery health indicators are capacity, and internal resistance. Internal resistance is a parameter directly correlated with the power the battery can deliver [5]. In this work, the capacity will be chosen as it is the most common one and can be used in most applications. Therefore the SOH is defined by :

$$SOH(t) = \frac{C(t)}{C_0} \tag{1}$$

where $C(t)$ represents the battery capacity in Ah at time t, and C_0 is its initial capacity in Ah.

B. Fuel cells & Electrolyzers

Fuel cells and electrolyzers are similar systems, as they have akin electrical behaviors (analogous polarization curves with activation, ohmic and concentration losses), and they both see their power characteristics deteriorate as they are used. Several indicators can be used to assess the loss of power, mainly the output voltage [7][8] and the internal resistance [9][10]. Ageing tests of fuel cells also demonstrated a modification of the polarization curve over time, that can be linked to the model of eq.2.

$$\begin{aligned} V_{st} =& n(E_0 - R_0(1+\alpha)i - AT\ln\left(\frac{\frac{i}{S}+j_{in}}{j_0}\right) \\ & - BT\ln\left(1 - \frac{\frac{i}{S}}{j_{L0}(1-\alpha)}\right) \end{aligned} \tag{2}$$

where V_{st} is the stack voltage [V], n is the number of cells in series, E_0 is the open-circuit voltage of a cell [V], R_0 is its resistance [Ω], i is the cell current [A], which is positive when hydrogen is consumed, S is the electrode surface [m^2], j_0 and j_L are its activation and limiting current densities [A/m^2] respectively, and A is the activation loss constant [V/K], j_{in} is the residual current density [A/m^2] and B is the concentration loss constant [V/K][11]. Here, α is the parameter that represents the ageing of a fuel cell during its life, and can be proportionally linked to the maximum power of the stack (Fig. 1)[12]. The SOH for fuel cells will therefore be defined as follows :

$$SOH(t) = 1 - \frac{\alpha(t)}{\alpha_{EoL}} \tag{3}$$

with α_{EoL} being the α value when the system reached its end-of-life. The rest of this work is made under the assumption that this SOH definition can be extended to the electrolyzers, as the equivalent voltage model (eq. 2) can be reversed for them and allows for a realistic

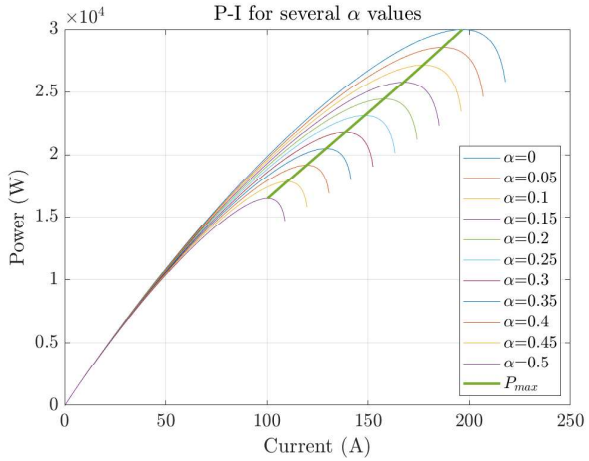

Fig. 1: Fuel cell power polarization curves during its lifetime

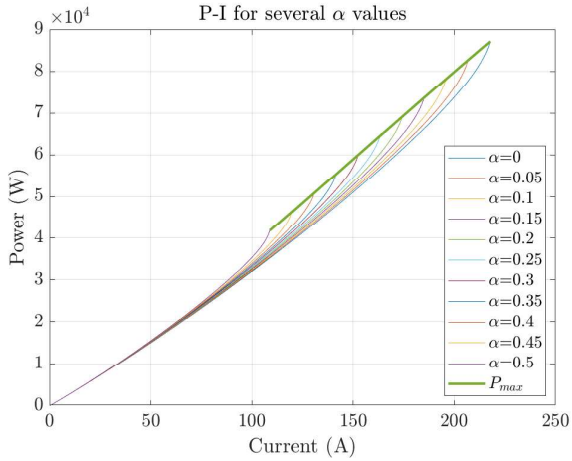

Fig. 2: Electrolyzer power polarization curves during its lifetime

polarization curve (see eq. 4 and fig. 2)[13].

$$V_{el} = n(E_0 + R_0(1+\alpha)i + AT\ln\left(\frac{\frac{i}{S} + j_{in}}{j_0}\right) + BT\ln\left(1 - \frac{\frac{i}{S}}{j_{L0}(1-\alpha)}\right) \quad (4)$$

Here the parameters have the same signification as in eq. 2, but now relative to the electrolyzer. The current is now considered to be positive when hydrogen is produced. It is worth noting that the focus of this work is made on the prognostic method, and that any timeserie could be used as input of the to be presented prognostics algorithm.

III. Prognostics approach

As the SOH of the different components have been defined, it is now assumed that the data about past SOH values are available and presented via a simple timeserie. If the diagnostic approach allows for the quantification of uncertainties, the mean data will be considered as the timeserie. There are several methods to obtain these SOH, such as electrochemical impedance spectroscopy (EIS) or current pulses for batteries [14][15][16], or filtering methods for fuel cells and electrolyzers [12][17].

A. State-of-the-art and algorithm choice

There are several methods that exist for SOH prognostic applications. They will aim to extrapolate ageing data from the SOH timeserie that is given as input. The first methods are the so-called model-based methods, which are therefore dependent on the system under study. They exist for various electrical systems, where they are mainly based on filtering algorithms [18]–[21]. The model-based methods offer several benefits, as they are often fast and quite simple to implement. However, they depend obviously largely on the system models they use, and therefore lack generality. The so-called data-driven methods allow to overcome these difficulties, but come at the cost of computation time. Among data-driven approaches, recurrent neural networks (RNNs) are the most common structures for applications to health state prediction in electrical energy storage components. The three main approaches among RNNs are Echo-State-Network (ESN)[22][23], Long Short-Term Memory (LSTM)[24][25] and transformers [26][27]. They can generally be classified in ascending order of complexity, with ESNs being the least heavyweight and least advanced structures, and transformers being the most complex structures, which are still for the moment the least used for health status prognostic applications. LSTMs is adopted in this work for their enhanced performance compared with ESNs, and for the greater relative maturity of this technology compared to transformers [28][29].

B. LSTM & Monte-Carlo dropout for prognostics

LSTM RNNs represent a powerful and sophisticated class of deep learning models. Their appeal lies in their ability to effectively process sequential data, such as sequences of text or timeseries in our case, while retaining long-term information. In contrast to traditional RNNs, LSTMs incorporate memory regulation mechanisms, enabling the gradient vanishing problem to be solved and long-term dependencies in sequences to be learned. To achieve this, LSTM networks are made of several cells which use two internal states, represented in Fig.3. The "cell" state represents the network's long-term memory, while the "hidden" state represents short-term memory. Both states interact with the input vector and each other. The output vector is then computed using the current hidden and cell states. The interest of LSTMs also lies in their ability to model complex temporal dependencies and capture patterns on different time scales. This makes them especially suitable for timeseries prediction. In addition, LSTMs are capable of autonomously learning hierarchical and abstract representations of sequential data, enabling them to make accurate predictions even in noisy or poorly structured environments, as it is the case in diagnostic approaches for estimating the health status of storage systems.

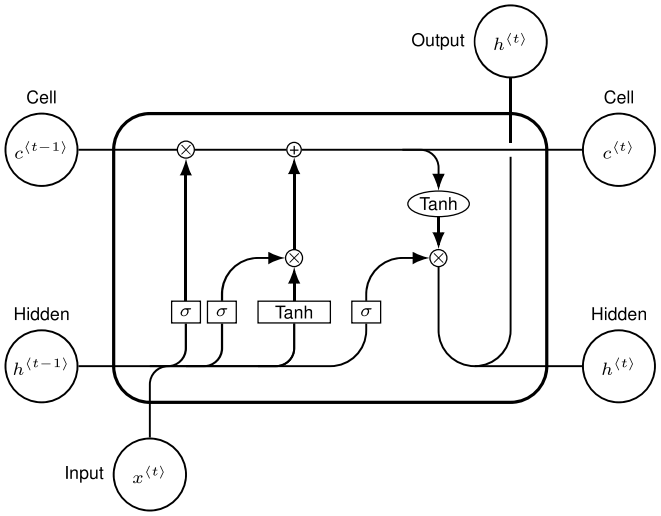

Fig. 3: Illustration of a LSTM cell

1) LSTM for timeseries prediction: A classic timeserie takes the form of a vector of n sequential data, the order of which is crucial. It is then common to separate this time series into a training part followed by a test part. This approach makes it possible to train the algorithm on the first part of the data and then check the neural network's correct prediction. It is common that the training data corresponds to the first 90% of the data, while the test data corresponds to the last 10% [30]. With this training set, it is useful to sequence it in order to create several input/output pairs for training purposes. Here, the inputs will correspond to sequences of data included in the training data. The length of these sequences (as a fraction of the total training data) will then be a crucial hyperparameter in the behavior of the neural network. The output corresponding to this sequence will then be the first value following this sequence. Data sequencing is summarized in Fig.4, where the T parameter determines the length of the sequence.

2) Algorithm hyperparameters: Next, the classical stochastic gradient descent method was used, with the optimization algorithm Adaptive Moment Estimation (adam), which is a standard method for this type of application. The loss function used was mean-squared error, which is also a standard approach. Then there are several hyperparameters that are crucial to the algorithm's operation:

- Initial data sampling affects prediction accuracy. Resampling with larger time steps reduces training time but may overlook short-term effects, useful for long-term predictions.
- The number of epochs, representing the number of times the training data is presented to the model, determines training duration. Too few may hinder convergence, while too many can lead to overfitting.
- Batch size, defining the number of data samples processed simultaneously during each iteration, also impacts learning speed. Larger batches may converge faster but risk local minima; smaller batches offer variability but may slow training.
- Sequence length, a percentage of training data, defines the temporal scope of each iteration. Longer sequences capture complex dependencies but increase computation time, while shorter ones may miss intricate patterns.
- Finally, the number of LSTM layers determines network depth, enhancing modeling but requiring more data and risking overfitting if not regularized.

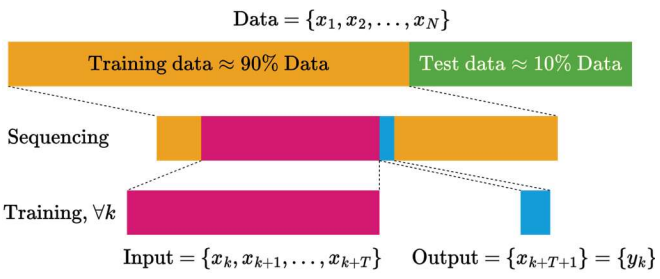

Fig. 4: Training data sequencing

In order to adjust these hyperparameters, it is possible to slice the training data even more finely to create a training set and a validation set. The presence of this validation set makes it possible to evaluate the loss function on these data during training, in order to identify any overfitting. Hyperparameters are then chosen such that the loss function on the validation set is minimized. All simulations are ran on Spyder® using Python.

3) Statistical approach using Monte Carlo Dropout: In the context of time series prediction, traditional approaches often rely on deterministic models, providing single predictions without explicit consideration of the associated uncertainty. However, these methods often ignore the natural variability and uncertainty inherent in temporal data, limiting their ability to provide a comprehensive assessment of predictions.
In this context, a statistical approach that explicitly incorporates uncertainty into predictions is highly desirable. The introduction of Monte Carlo Dropout stems from this need to estimate uncertainty in time series predictions in a statistically robust way. This approach is based on the idea of dropout, a regularization method that consists of randomly deactivating certain neuron links during the training of a neural network. By applying the dropout stochastically during the prediction phase, Monte Carlo Dropout generates a set of stochastic predictions. By repeating this process a large number of times, it is possible to collect a distribution of predictions, enabling the uncertainty associated with each predicted point to be estimated.
This approach offers a valuable statistical perspective by providing confidence intervals and probabilistic estimates, enabling a more comprehensive and reliable assessment of time series predictions. In this work, dropout is controlled via the `recurrent_dropout` parameter of the `tensorflow` library, which has the effect of

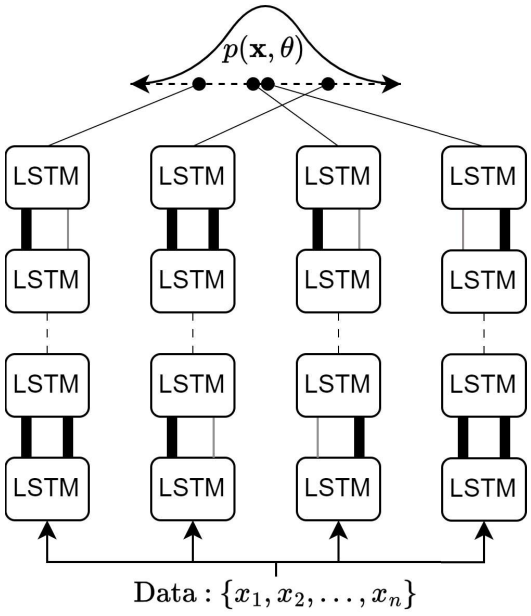

Fig. 5: Illustration of the introduction of dropout (thin links) in an LSTM network (4 vertical networks)

randomly resetting (with a probability corresponding to its corresponding frequency) the connections between LSTM layers. This corresponds to randomly ignoring recurring connections between LSTM cells, and applies to the "cell" and "hidden" links in Fig.3. A schematic diagram of how dropout is used in this context is given in Fig.5.

C. Results

As for the results, several timeseries have been used as input to assess the versatility of the algorithm. A first timeserie from an open dataset of 18650 NMC battery degradation has been used for the prognostics applied to batteries [31].

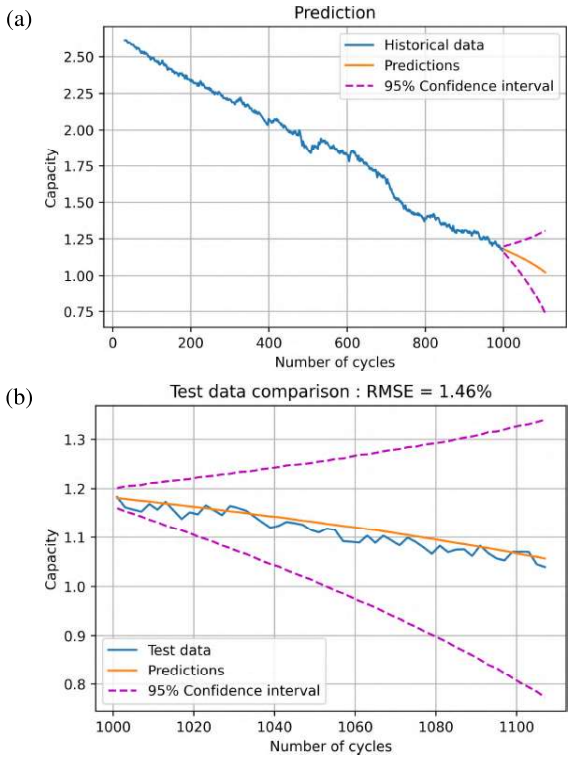

Fig. 7: (a) Prediction and (b) comparison with test data for capacity prediction

The small local capacity increases can be explained by various noise factors in the acquisition (or rest times, temperature changes...) and are not considered significant. A second timeserie for fuel cells and electrolyzers has been manually generated to depict the evolution of the α parameter. The detail of this generation can be found in work [32]. A third timeserie made from a simple growing sine wave with added noise is also included to evaluate the network's generalization capacity (Fig. 6). All these three timeseries have been served as inputs for the neural network. The hyperparameters are set as described in section III-B2, which resulted in a sequence

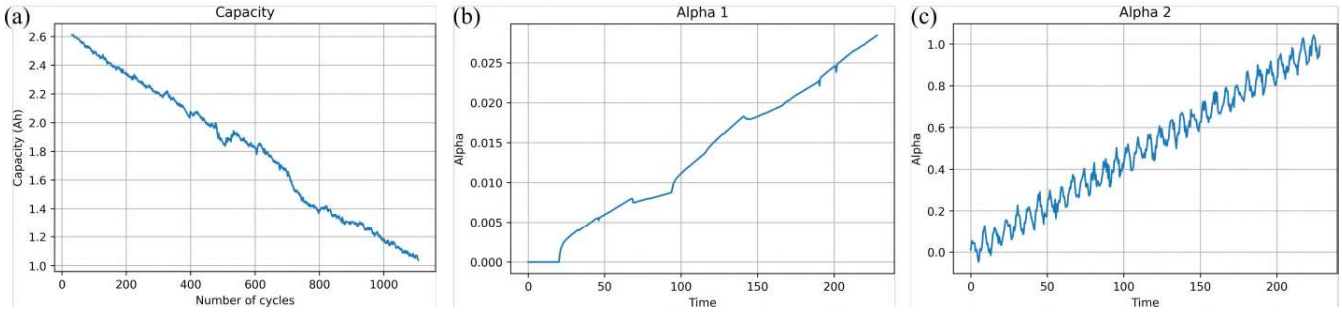

Fig. 6: SOH timeseries used as input for LSTM prediction ((a) battery capacity, (b) FC/ELY alpha 1, (c) FC/ELY alpha 2)

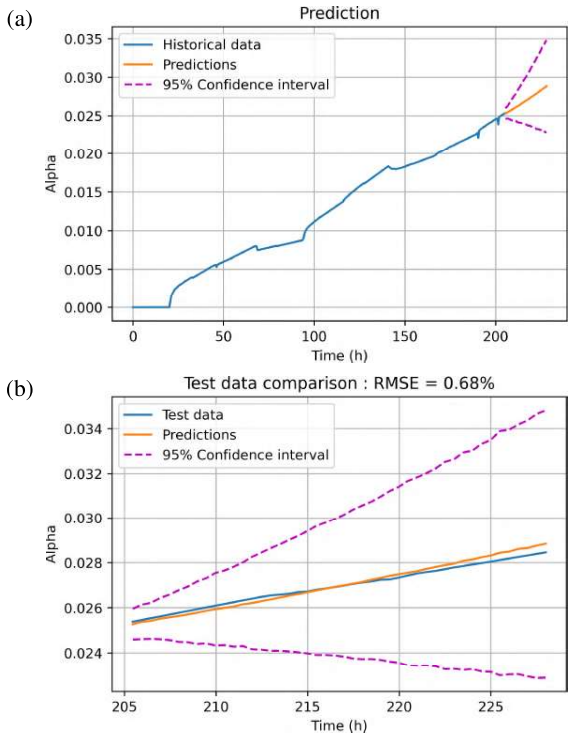

Fig. 8: (a) Prediction and (b) comparison with test data for first α prediction

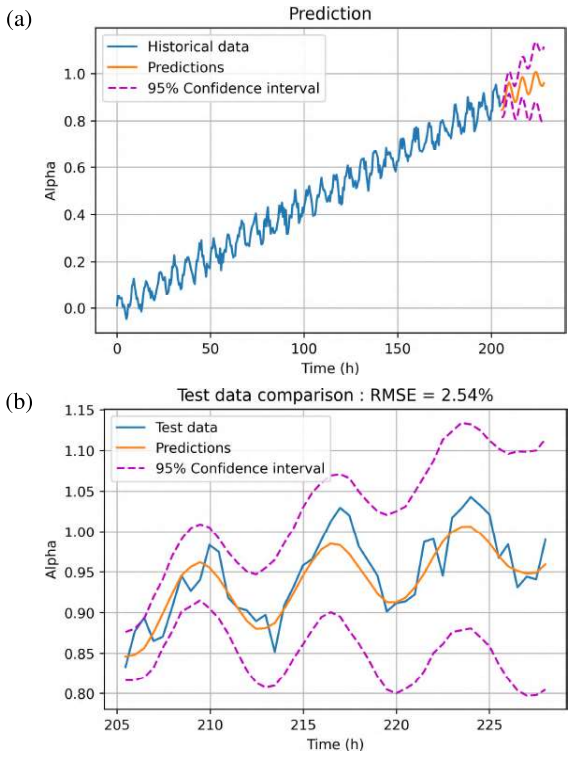

Fig. 9: (a) Prediction and (b) comparison with test data for second α prediction

comprising $2/3$ of the training data and a sampling time that yielded approximately 800 data points per timeseries, representing a compromise between long-term vision and accounting for local variations. A total of 100 different networks for Monte-Carlo dropout are used with a dropout parameter of 0.2. The results for the capacity are presented in Fig.7, while the results for the two α profiles are respectively shown in Fig.8 and 9. On each figure, the prediction is first presented, with its corresponding confidence interval provided by the Monte-Carlo dropout. A comparison with the test data is also provided, along with the RMSE demonstrating the closeness between the prediction and the reality. All three predictions have great similarities with the data, assessing the effectiveness of the neural network. The fact that the network performed well on these three types of series confirmed its generalization capacity. From this study, it is then possible to obtain the Remaining-Useful-Life (RUL) of the considered systems, by comparing the projected evolution of the SOHs with the end-of-life (EOL) criteria. The confidence interval can also be used for the RUL study, and a 95% lower bound can be deduced. It is however impossible to get a RUL upper bound from this projection, as the confidence interval starts to increase (for the capacity) or decrease (for the α) when the prediction starts, therefore never crossing the EOL threshold. This marks a limitation of this approach.

IV. Conclusion

In this paper, a novel versatile approach for the prognostics of energy storage systems has been presented. This prognostics approach is based on the extrapolation of states-of-health (SOHs) timeseries, in order to derive a remaining useful life (RUL) parameter. This work is made with the aim of building an ageing tolerant energy management strategy. The SOHs of the energy storage components were first introduced, using a novel indicator for the hydrogen storage systems that was yet to be used through extrapolation. The recurrent neural network approach was then presented through a brief state-of-the-art, and the Long Short-Term Memory (LSTM) algorithm was adopted as the best compromise between performance and reliability. Monte-Carlo dropout was used as a way to quantify uncertainties, and results on three different timeseries were then presented. The algorithm's ability to adapt to each timeserie showed its versatility, and therefore its relevance in prognostics for various energy storage systems. This paper aims to be completed by further work on advanced energy management strategies that would take into account

the evolution of the SOHs for predictive maintenance applications.

References

[1] H. Ritchie and P. Rosado, "Electricity mix," *Our World in Data*, 2020.

[2] J. Vetter, P. Novák, M. R. Wagner, *et al.*, "Ageing mechanisms in lithium-ion batteries," *Journal of Power Sources*, vol. 147, no. 1, pp. 269–281, Sep. 9, 2005.

[3] L. Dubau, L. Castanheira, F. Maillard, *et al.*, "A review of PEM fuel cell durability: Materials degradation, local heterogeneities of aging and possible mitigation strategies," *WIREs Energy and Environment*, vol. 3, no. 6, pp. 540–560, 2014.

[4] G. Papakonstantinou, G. Algara-Siller, D. Teschner, T. Vidaković-Koch, R. Schlögl, and K. Sundmacher, "Degradation study of a proton exchange membrane water electrolyzer under dynamic operation conditions," *Applied Energy*, vol. 280, p. 115 911, Dec. 15, 2020.

[5] N. Noura, L. Boulon, and S. Jemeï, "A review of battery state of health estimation methods: Hybrid electric vehicle challenges," *World Electric Vehicle Journal*, vol. 11, no. 4, p. 66, Dec. 2020.

[6] C. Zhang, Y. Zhang, L. Wang, X. Deng, Y. Liu, and J. Zhang, "A health management review of proton exchange membrane fuel cell for electric vehicles: Failure mechanisms, diagnosis techniques and mitigation measures," *Renewable and Sustainable Energy Reviews*, vol. 182, p. 113 369, Aug. 1, 2023.

[7] F. Harel. "Défi ieee phm data 2014." (2021).

[8] X. Yan, C. Locci, F. Hiss, and A. Nieße, "State-of-health estimation for industrial h2 electrolyzers with transfer linear regression," *Energies*, vol. 17, p. 1374, Mar. 13, 2024.

[9] R. Pan, D. Yang, Y. Wang, and Z. Chen, "Health degradation assessment of proton exchange membrane fuel cell based on an analytical equivalent circuit model," *Energy*, vol. 207, p. 118 185, Sep. 15, 2020.

[10] S. Khurana, D. M. Hall, R. S. Schatz, M. V. Fedkin, and S. N. Lvov, "State-of-health of a CuCl electrolyzer during a 168-h test," *International Journal of Hydrogen Energy*, vol. 40, no. 1, pp. 62–69, Jan. 5, 2015.

[11] S. Kong, M. Bressel, M. Hilairet, and R. Roche, "Advanced passivity-based, aging-tolerant control for a fuel cell/super-capacitor hybrid system," *Control Engineering Practice*, vol. 105, p. 104 636, Dec. 1, 2020.

[12] M. Bressel, M. Hilairet, D. Hissel, and B. Ould Bouamama, "Extended kalman filter for prognostic of proton exchange membrane fuel cell," *Applied Energy*, vol. 164, pp. 220–227, Feb. 2016.

[13] E. Urbano, E. Pahon, N. Yousfi-Steiner, and M. Guillou, "Accelerated stress testing in proton exchange membrane water electrolysis - critical review," *Journal of Power Sources*, vol. 623, p. 235 451, Dec. 15, 2024.

[14] B. Li, H. Qu, M. Zhou, and D. Jiang, "Online measurement method of electrochemical impedance of electric vehicle battery based on three-phase motor drive inverter," in *2023 25th European Conference on Power Electronics and Applications (EPE'23 ECCE Europe)*, Sep. 2023, pp. 1–6.

[15] S. Vaidya, D. Depernet, D. Chrenko, and S. Laghrouche, "Experimental development of embedded online impedance spectroscopy of lithium-ion batteries – proof of concept and validation," in *ELECTRIMACS 2022*, S. Pierfederici and J.-P. Martin, Eds., Cham: Springer International Publishing, 2024, pp. 67–83, ISBN: 978-3-031-55696-8.

[16] S. Jin, X. Yu, X. Sui, W. Guo, M. Berecibar, and D.-I. Stroe, "Features extraction for battery SOH estimation from battery pulsed charging operation," in *2023 25th European Conference on Power Electronics and Applications (EPE'23 ECCE Europe)*, Sep. 2023, pp. 1–7.

[17] P. Wang, H. Liu, J. Chen, *et al.*, "A novel degradation model of proton exchange membrane fuel cells for state of health estimation and prognostics," *International Journal of Hydrogen Energy*, vol. 46, no. 61, pp. 31 353–31 361, Sep. 3, 2021.

[18] S. Kim, H. J. Park, J.-H. Choi, and D. Kwon, "A novel prognostics approach using shifting kernel particle filter of li-ion batteries under state changes," *IEEE Transactions on Industrial Electronics*, vol. 68, no. 4, pp. 3485–3493, Apr. 2021.

[19] M. Ahwiadi and W. Wang, "An enhanced particle filter technology for battery system state estimation and RUL prediction," *Measurement*, vol. 191, p. 110 817, Mar. 15, 2022.

[20] Y. Ao, S. Laghrouche, D. Depernet, and K. Chen, "Proton exchange membrane fuel cell prognosis based on frequency-domain kalman filter," *IEEE Transactions on Transportation Electrification*, vol. 7, no. 4, pp. 2332–2343, Dec. 2021.

[21] A. Vulli, G. Schlottig, M. Orkisz, M. Firla, and E. Bianda, "A model-based approach for prognostics of power semiconductor modules," in *2023 25th European Conference on Power Electronics and Applications (EPE'23 ECCE Europe)*, Sep. 2023, pp. 1–10.

[22] M. Catelani, L. Ciani, R. Fantacci, G. Patrizi, and B. Picano, "Remaining useful life estimation for prognostics of lithium-ion batteries based on recurrent neural network," *IEEE Transactions on Instrumentation and Measurement*, vol. 70, pp. 1–11, 2021.

[23] M. Yue, Z. Li, R. Roche, S. Jemei, and N. Zerhouni, "Degradation identification and prognostics of proton exchange membrane fuel cell under dynamic load," *Control Engineering Practice*, vol. 118, p. 104 959, Jan. 1, 2022.

[24] L. Zhang, T. Ji, S. Yu, and G. Liu, "Accurate prediction approach of SOH for lithium-ion batteries based on LSTM method," *Batteries*, vol. 9, no. 3, p. 177, Mar. 2023.

[25] C. Wang, Z. Li, R. Outbib, M. Dou, and D. Zhao, "A novel long short-term memory networks-based data-driven prognostic strategy for proton exchange membrane fuel cells," *International Journal of Hydrogen Energy*, vol. 47, no. 18, pp. 10 395–10 408, Feb. 28, 2022.

[26] D. Chen, W. Hong, and X. Zhou, "Transformer network for remaining useful life prediction of lithium-ion batteries," *IEEE Access*, vol. 10, pp. 19 621–19 628, 2022.

[27] J. Lv, Z. Yu, H. Zhang, G. Sun, P. Muhl, and J. Liu, "Transformer based long-term prognostics for dynamic operating PEM fuel cells," *IEEE Transactions on Transportation Electrification*, vol. 10, no. 1, pp. 1747–1757, Mar. 2024.

[28] R. Chandra, S. Goyal, and R. Gupta, "Evaluation of deep learning models for multi-step ahead time series prediction," *IEEE Access*, vol. 9, pp. 83 105–83 123, 2021.

[29] H. Hewamalage, C. Bergmeir, and K. Bandara, "Recurrent neural networks for time series forecasting: Current status and future directions," *International Journal of Forecasting*, vol. 37, no. 1, pp. 388–427, Jan. 1, 2021.

[30] X. Li, K. Xiao, X. Li, C. Yu, D. Fan, and Z. Sun, "A well rate prediction method based on LSTM algorithm considering manual operations," *Journal of Petroleum Science and Engineering*, vol. 210, p. 110 047, Mar. 1, 2022.

[31] "Cycle test data." (2021), [Online]. Available: https : / / database . batteryarchive . org / public / dashboards / 61PzyYn9u56njtPDOh37VVBFasGusUlxc7WZ1FSj?org_slug = default & p_cell_id = %5C % 5B % 5C % 22HNEI_18650_NMC_LCO_25C_0 - 100_0 . 5 % 5C % 2F1 . 5C_a % 5C % 22 % 5C % 5D & p_w21_Step_1 = 100 & p_w21_Step_2 = 2 & p_w21_Step_3 = 1000 & p_w22_Step_1 = 2 & p_w22_Step_2=100&p_w22_Step_3=1000.

[32] T. Lenoir, D. Chrenko, R. Roche, S. Jemei, and M. Hilairet, "Diagnostic d'une PEMFC dans un micro-réseau électrique DC par représentation énergétique macroscopique pour des applications de jumelage numérique," in *Conférence des Jeunes Chercheurs en Génie Électrique*, Le Croisic, France, Jun. 2024.